

Two-Dimensional Spin-Diffusion NMR Reveals Differential Mixing in Biodegradable Polymer Blends

Xin Jia, Xingwu Wang,[†] A. E. Tonelli,[†] and Jeffery L. White*

Department of Chemistry, North Carolina State University, Raleigh, North Carolina 27695

Received October 19, 2004; Revised Manuscript Received January 17, 2005

ABSTRACT: Length scales of mixing in amorphous blends of solid PCL (polycaprolactone) and PLLA (poly-L-lactic acid) were investigated as a function of preparation method. A recently described two-dimensional heteronuclear correlation (Hetcor) spin-diffusion technique (Jia et al. *Macromolecules* 2003, 36, 712) revealed that PCL/PLLA blends with shorter length scales of mixing, relative to solution blending, could be prepared using inclusion-compound coalescence methods (Rusa et al. *Macromolecules* 2000, 33, 5321). These biocompatible and biodegradable polymer blends provide a clear example of the utility of the 2D Hetcor spin-diffusion method for quantitative miscibility and phase analysis in amorphous macromolecules and their blends. The rates for intrapolymer polarization transfer vs interchain/interdomain polarization equilibration were easily differentiated using the 2D technique for either blend. As a result, spin-diffusion coefficients and miscibility length scales could be calculated by direct measurement on the blend constituents, while more traditional methods involving NMR relaxation proved inconclusive.

Introduction

Characterization of amorphous mixtures is central to intelligent design and application of multicomponent materials, including inorganic glasses, organic polymers, or composites containing both organic and inorganic constituents.¹ Understanding structure in these “disordered” systems is constrained by the obvious limits on diffraction experiments, and optical, electron, or neutron scattering often suffer from insufficient contrast for mixtures of chemically similar materials. Blends of biodegradable polymers, such as aliphatic polyesters, are a typical example of targeted amorphous mixtures whose physical properties are currently deficient relative to more established polyolefins.² Optimization of physical properties in biodegradable polymers, and the resulting environmental benefits from new commercial applications, is hampered by the lack of molecular- and meso-scale characterization data on the end-use polymer mixtures. Magnetic resonance has proved useful in the analysis of phase behavior in many amorphous polymer systems, since several types of experiments can provide mixing scale information without having to dissolve the macromolecules, incorporate isotopic labels, or synthetically incorporate contrast agents.^{3–5} In general, there are distinct characteristics common to the polymers in most previously published reports where NMR successfully characterized bulk mixing behavior. The individual blend constituents possessed either (1) significantly different values of T_g and, therefore, differential chain dynamics in the blend, (2) different relaxation rates (e.g., T_1 , $T_{1\rho}$, or T_2), or (3) a large range of ^1H chemical shifts in their NMR spectra (e.g., both aliphatic and olefinic/aromatic). While variable-temperature experiments may improve spectroscopic contrast in systems that do not exhibit sufficiently disparate values in any of these categories, such changes are often incongruent

with critical solution temperatures for the mixture. Therefore, a clear need exists for generally applicable methods to determine mixing length scales in amorphous blends of polymers with similar chemical, physical, and spectroscopic properties.

In this contribution, we describe the extension of a previously published experimental approach to such a class of materials.⁶ Specifically, we prepare binary, amorphous polymer blends of PCL (polycaprolactone) and PLLA (poly-L-lactic acid), using two different preparation methods. These aliphatic polyesters are important candidates for economically viable biodegradable polymers and in addition offer the promise of biocompatibility. PCL has high flexibility with low tensile strength. Its melting point is 60 °C, and it has a glass transition temperature of –40 °C. On the other hand, PLLA has a high tensile strength, high melting point (ca. 160 °C), and a relatively high $T_g = 60$ °C. Because of its high crystallinity, PLLA is very brittle with low elongation at break. Separately, neither polymer offers attractive performance attributes. Together, as a compatible blend, they may produce a sufficiently tough but pliable biopolymer suitable for a variety of pharmaceutical, biomedical, and environmental applications.^{7–9} However, PCL and PLLA are incompatible and phase separate when prepared using simple solution or melt-blending methods. Recently, Rusa and co-workers have shown that compatibility in PCL–PLLA blends is enhanced using inclusion-compound coalescence methods.¹⁰ However, quantitative proof of the length scales of mixing in solution vs inclusion-compound blending methods was not reported.

This contribution shows that two-dimensional spin-diffusion NMR experiments indicate reduced length scales of mixing via the inclusion compound coalescence method, i.e., enhanced compatibility for this PCL/PLLA blend. The PCL/PLLA system is an excellent representative example of a blend in which the constituents have similar NMR relaxation properties, similar chain dynamics once they are blended, and a relatively small ^1H chemical shift dispersion. In addition, there is a clear

[†] Fiber and Polymer Science Department, North Carolina State University.

* To whom all correspondence should be addressed. E-mail: Jeff_L_White@ncsu.edu.

connection between the practical utility of this amorphous blend as a biocompatible/biodegradable material and subtle differences in its morphology. Permeability and biodegradation rates govern selection of controlled-drug delivery candidates, as well as general environmental reclamation concerns, and these in turn depend on the morphological details of blends.⁹ As such, the general applicability of the two-dimensional spin-diffusion technique to important mixing problems in polymer science is clearly demonstrated.

Experimental Section

Sample Preparation. PCL and PLLA were each synthesized at 115 °C by ring-opening polymerization of ϵ -caprolactone and L-lactide (both from Aldrich), respectively.⁹ Syntheses were carried out in toluene, with 1-dodecanol and SnOct (ca. 0.1% of monomer in molar amount) used as the initiator and catalyst, respectively. Polymers were purified by cold methanol precipitation, followed by drying at 40 °C in a vacuum oven for 48 h. Both polymers had $M_n \approx 10\,000$ g/mol, with polydispersity ≈ 1.2 . Blend preparation by solution was accomplished by dissolving an equimolar mixture of each polymer in dioxane to generate a ca. 2–5 wt % solution of the polymers, followed by precipitation with water. Preparation of PCL–PLLA blends via coalescence from their inclusion compounds with cyclodextrin in acetone has been described in detail previously, and the identical method was used in this case.¹⁰ Briefly, the coalesced PCL–PLLA blend was obtained by washing the inclusion compounds with DMSO, followed by subsequent drying in a vacuum oven for a minimum of 48 h.

Characterization of the coalesced PCL–PLLA blend by polarizing microscopy, DSC, and X-ray diffraction revealed that $\leq 5\%$ crystallinity was present in the blend and that no distinct morphology or domain structure was present. In contrast, distinct PCL and PLLA diffraction peaks remained for the dioxane-cast blend, suggestive of a longer length scale of mixing with residual regions of both PCL and PLLA crystallinity ($\sim 45\%$ for each).

Solid-State NMR Methods. All the solid-state NMR experiments were performed on a Bruker DSX-300 instrument using 4 mm zirconium oxide rotors, operating at a field strength of 7.05 T, corresponding to a 300 MHz ^1H Larmor frequency. ^1H Bloch decay spectra were acquired using magic angle spinning (MAS) speeds of 4 and 13 kHz and a $3.5\ \mu\text{s}$ $\pi/2$ pulse width. ^{13}C cross-polarization/magic angle spinning pulse sequence (CP/MAS), $T_1(\text{H})$, $T_{1\rho}(\text{H})$ measurements were performed with 3–4 kHz MAS and 3–3.5 μs $\pi/2$ pulse width. Radio-frequency field strengths for ^1H decoupling, unless otherwise specified, were 70–73 kHz. The cross-polarization contact time was 1 ms, and the delay between two consecutive scans was 2–4 s. ^1H T_1 's were measured via ^{13}C detection using the combination of cross-polarization and saturation-recovery pulse sequence, while ^1H $T_{1\rho}$'s were acquired using a cross-polarization pulse sequence preceded by a variable proton spin-lock period.

The two-dimensional (2D) ^1H – ^{13}C spin diffusion heteronuclear correlation (Hetcor) data were obtained using two different experimental techniques, with similar results obtained by each. The multiple-pulse windowless isotropic mixing Hetcor (MP/WIM) sequence first reported by Burum et al.,¹¹ as well as a 2D frequency switched Lee–Goldburg with Lee–Goldburg cross-polarization (2D FSLG/LGCP), were used to obtain the 2D solid-state heteronuclear correlation data reported here.¹² Specific parameters for the MP/WIM Hetcor experiments are identical to those used in our previous study but briefly include $\pi/2$ pulse widths = $3.2\ \mu\text{s}$ on each channel and MAS speeds = 4 kHz, and insertion of controlled periods of ^1H – ^1H spin diffusion was introduced prior to the isotropic $^1\text{H}/^{13}\text{C}$ polarization transfer step. For the FSLG/LGCP Hetcor data, the heteronuclear polarization transfer (CP time = 100 μs) under ^1H Lee–Goldburg conditions, and 12 kHz MAS, ensures that homonuclear ^1H spin diffusion does not occur during the CP contact period. The ^1H radio-frequency field

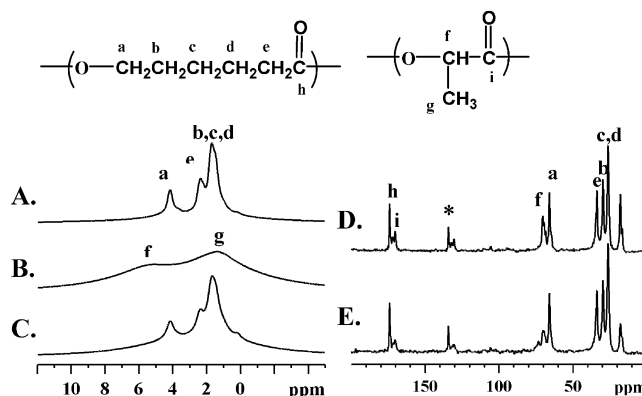


Figure 1. (A) ^1H Bloch decay spectrum of pure bulk PCL. (B) ^1H Bloch decay of pure bulk PLLA. (C) ^1H Bloch decay of coalesced PCL/PLLA blend. (D) ^{13}C CP/MAS spectrum for the solution PCL/PLLA blend. (E) ^{13}C CP/MAS spectrum for the same sample as in (C). Assignments follow the structure schematic (top). Spectra A–C were acquired with 12 kHz MAS. Asterisks denote spinning sidebands.

strength during the FSLG evolution period and TPPM decoupling period were set at ca. 95 kHz. Quadrature detection in t_1 was achieved by time proportional phase incrementation (TPPI) for each Hetcor method. In all cases, experimental verification of proper Hetcor calibration was done using monoethyl fumarate.¹³ Spin-diffusion curves were constructed by extracting individual ^1H slices in the second dimension and quantitatively deconvoluting the appropriate intensity ratios using PeakFit.

Simulation of Polymer Chain Units. Characteristic monomer sizes for spin-diffusion were determined via molecular dynamics calculation and dimensional measurements on PLLA and PCL chains with degrees of polymerization = 99, using the Insight II molecular modeling package (Polymer version 3.0.0) with PCFF force field parameters running on a Silicon Graphics IRIS Indigo workstation. Energy minimization was computed with 5000 iterations of an adjusted-basis steepest-descent algorithm. Dynamics simulations were carried out at constant temperature of 300 K for 5 ps with time step of 1 fs. The minimum distance between pendant CH_3 protons and the OCH proton on the backbone (0.25 nm) defines the average PLLA monomer size for intramolecular ^1H spin-diffusion, since these are the only two unique PLLA protons present; an identical distance was calculated trigonometrically. PCL, which has a more complicated structure containing several different proton types, was found to have a characteristic monomer size $x = 0.38$ nm using a similar structure simulation routine. Details of the calculation for characteristic monomer dimensions have been described previously.⁶

Results and Discussion

One-Dimensional ^1H and ^{13}C Solid-State NMR Analysis. Figure 1 shows ^1H one-pulse spectra for the solid, coalesced PCL–PLLA blend, obtained at 30 °C using 13 kHz MAS. Identical spectra were collected using 4 kHz MAS (not shown). Examination of the spectra and structure assignments reveals that (1) the total resolvable chemical shift separation is less than 3 ppm, (2) the peak widths are large, and (3) no resolved signals exist in the blend by which one can differentiate PCL and PLLA protons (Figure 1C). These spectral characteristics render difficult the use of direct ^1H spin-diffusion methods for quantitative interrogation of phase behavior in the blends. The ^1H spectrum for the solution blend (not shown) is identical to the coalesced blend. In contrast, the ^{13}C CP/MAS spectra in Figure 1D,E show well-resolved signals for each carbon type originating from both PCL and PLLA, including the

Table 1. ^1H Rotating-Frame Spin-Lattice Relaxation Time Constants $T_{1\rho\text{H}}$ (in ms) for PCL/PLLA Blends vs Sample Preparation Method

peak (ppm)	pure PCL (ms)	pure PLLA (ms)	solution blend (ms)	coalesced (ms)
67	62.9		70.6	49.9
30	38.9		47.7	38.6
27	32.6		37.8	37.6
71		38.7	30.1	40.2
19		25.2	42.3	45.3

Table 2. ^1H Spin-Lattice Relaxation Time Constants T_1 (in s) for PCL/PLLA Blends vs Sample Preparation Method

peak (ppm)	pure PCL (s)	pure PLLA (s)	soution blend (s)	coalesced (s)
67	1.67		1.04	0.88
30	1.78		1.04	0.86
27	1.88		1.02	0.85
71		1.20	0.74	0.77
19		1.20	0.84	0.98

aliphatic signals from the ester linkage (65–75 ppm). Poorly resolved ^1H spectra, but well-resolved ^{13}C data, are common in solid polymers, and ^{13}C detection of the ^1H spin-lattice ($T_{1\text{H}}$) and rotating-frame ($T_{1\rho\text{H}}$) relaxation times routinely provides a mechanism to discern length scales of mixing.^{3–5} However, this requires that the individual relaxation times be sufficiently distinct (typically to a factor of ≥ 2) to obtain accurate domain size information.⁵

Tables 1 and 2 show that the ^1H relaxation times for the individual blend components are too similar to reliably extract mixing dimensions. In addition, we observe from Table 1 that $T_{1\rho\text{H}}$ values are different even within the pure polymers, further complicating the use of $T_{1\rho\text{H}}$ values for length scale of mixing calculations in this case and also demonstrating the danger of this approach for blends of mobile polymers unless the temperature is reduced significantly.¹⁴ Finally, we note that attempts were made to exploit ^1H T_2 differences to selectively eliminate all of the ^1H magnetization from either the PCL or the PLLA component in the coalesced blend, which would have allowed spin-diffusion measurements using either ^1H - or ^{13}C -detected dipolar filter experiments.^{15,16} Such experiments were unsuccessful, as all peaks in the ^1H and ^{13}C spectra were equally attenuated with increasing filter cycle strength (data not shown).

Two-Dimensional Spin-Diffusion NMR. The constraints discussed above suggest that the PCL/PLLA blend system is an ideal candidate for analysis using 2D Hetcor methods.^{17–19} We have previously demonstrated that this technique can independently determine spin-diffusion coefficients and length scale of mixing in polymers and copolymers, since both polarization equilibration within monomeric units and between distinct polymer domains may be resolved.⁶ Representative 2D spin-diffusion Hetcor plots are shown in Figure 2 for the coalesced and solution-cast blends. While many plots (>30) were obtained using both types of Hetcor pulse sequences with several spin-diffusion times, only a small subset of the data is shown in Figure 2 for brevity. Figures 2A,B and 2C,D illustrate that identical results were obtained using both the FSLG/LGCP and MP/WIM Hetcor sequences, and as expected on the basis of the results of Figure 1, the ^1H line shapes are broad in the second dimension for this amorphous system. Extraction of ^1H slices as a function of mixing time at the PLLA

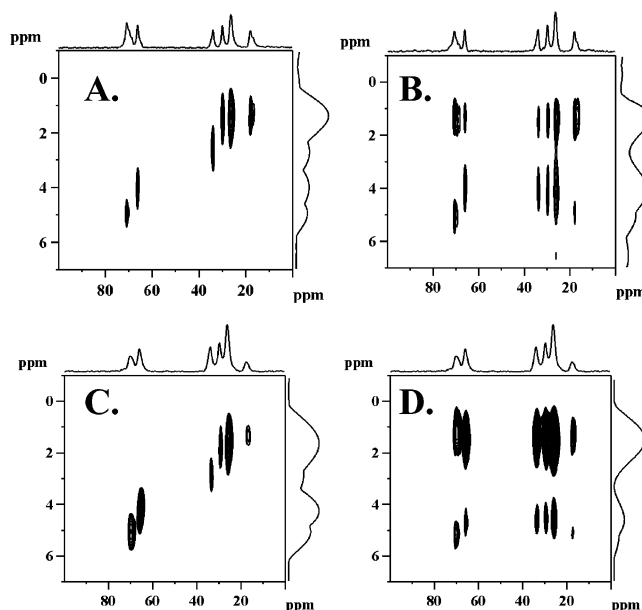


Figure 2. Representative two-dimensional ^1H – ^{13}C solid-state Hetcor plots of the aliphatic ^{13}C region for (A) FSLG/LGCP acquisition on the solvent-cast blend with no spin-diffusion time; (B) same as (A), after 1 ms spin-diffusion time; (C) MP/WIM acquisition on the coalesced blend with no spin-diffusion time; and (D) same as (C), after 1 ms mixing time. ^1H slices were extracted at 19 and 65 ppm for the spin-diffusion analysis. Summed projections from each dimension are shown along the ^{13}C (horizontal) and ^1H (vertical) axes.

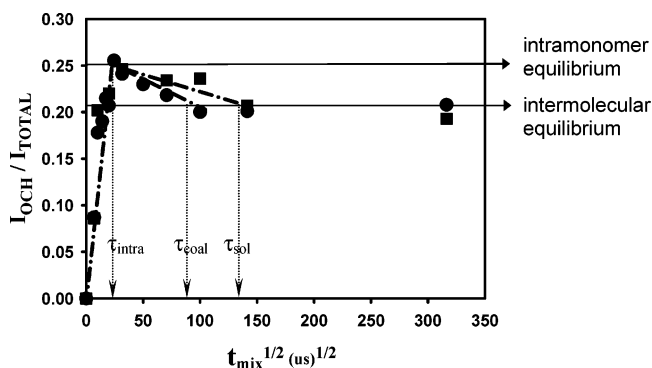


Figure 3. ^1H spin-diffusion curves extracted from slices at the PLLA CH_3 signal (19 ppm) for the solution-cast (■) and coalesced (●) PCL/PLLA blends. The horizontal arrows indicate the predicted equilibrium intensity ratios for intramonomer vs intermolecular (interdomain) spin-diffusion based on the monomer structures. The dashed line in the short time regime is the regression through the first five points of the curve to the intramolecular equilibrium intensity ratio (0.25). From this latter analysis, the equilibration time for intramolecular spin-diffusion was $20 \mu\text{s}^{1/2}$ (τ_{intra} vertical arrow). Additional vertical arrows indicate the equilibration times for intermolecular or interdomain spin-diffusion between PLLA and PCL in the coalesced ($\tau_{\text{coal}} = 88 \mu\text{s}^{1/2}$) and solution-cast ($\tau_{\text{sol}} = 132 \mu\text{s}^{1/2}$) blends, obtained by regression of the four experimental points between the intramolecular and intermolecular plateaus.

CH_3 (19 ppm) and the PCL OCH_2 (65 ppm) ^{13}C peaks provided the necessary time-dependent data for quantitative spin-diffusion analysis.

Quantitative analysis of the ^1H slices extracted from the Hetcor data represented by Figure 2 over the full range of spin-diffusion times produced the spin-diffusion curves shown in Figure 3 for the coalesced vs the solvent-cast PCL/PLLA blends. Again, the method of slice extraction and deconvolution has been previously

discussed in detail.⁶ The intensity ratio plotted on the ordinate of Figure 3 is simply the fraction of the OCH_x region (4–6 ppm) intensity relative to the total intensity in the ¹H slice at the PLLA CH₃ peak position (19 ppm) in the ¹³C dimension.

Figure 3 shows that the experimental results for the intensity distribution in the ¹H slice follow our expectation based on the monomer structures. More importantly, a well-defined intramolecular spin-diffusion equilibrium point is observed, the absolute intensity ratio for which (0.25) is larger than that for complete polarization redistribution among both polymers in the blend (0.21). Referring back to the structures and spectra in Figure 1, we observe that the extraction of ¹H slices at the PLLA CH₃ ¹³C peak as a function of spin-diffusion time is tantamount to following the propagation of methyl proton polarization first within the PLLA monomer (intramolecular equilibrium) and then to neighboring chains (intermolecular equilibrium). Ultimately, that magnetization is distributed, and mixed, between both PCL and PLLA protons according to the stoichiometric values from the monomer structures and the overall blend composition. As such, at final equilibrium the ¹H slice has two broad peaks reflecting the combined ester (3 protons contributing to the 3.5–5.5 ppm region) and aliphatic hydrogens (11 protons contributing to the 1–3.5 ppm). In summation, the intensity from 3 ester protons relative to the total 14 protons in the system gives the 0.21 value for intermolecular equilibration, as expected for the equimolar blend compositions.

Initial rate analysis of the first five data points in Figure 3 with respect to the intramolecular equilibrium ratio yields a value for the PLLA intramolecular time ($\tau_{\text{intra}}^{1/2} = 20 \mu\text{s}^{1/2}$).²⁰ This spin-diffusion time, along with the characteristic monomer dimension x from the structure simulation (see Experimental Section), can be used to determine the spin-diffusion D coefficient via solution of the diffusion equation $D = (\pi x^2)/(4\tau_{\text{intra}})$.²¹ From this, we determine $D = 1.1 \times 10^{-12} \text{ cm}^2 \text{ s}^{-1}$ for PLLA in the coalesced blend ($D_{\text{PLLA}}^{\text{coal}}$). An important point to note is that this spin-diffusion coefficient $D_{\text{PLLA}}^{\text{coal}}$ was determined by direct measurement on PLLA in the environment of interest, did not require reference to any other measurement technique or reference polymer, and may not be equal to the D value for pure PLLA (vide infra). As we have previously discussed, the intramolecular model for any given polymer defines a quantitative upper limit on the value of D .⁶

Figure 3 shows that intermolecular polarization transfer reaches the equilibrium condition much faster for the coalesced blend compared to the solution blend ($\tau_{\text{coal}}^{1/2} = 88 \mu\text{s}^{1/2}$ vs $\tau_{\text{sol}}^{1/2} = 132 \mu\text{s}^{1/2}$, respectively), proving that the average distance between PLLA-rich and PCL-rich regions is significantly smaller in their blends prepared by coalescence from the cyclodextrin inclusion compound. From Figure 3, and using a modified form of the diffusion equation appropriate for a binary mixture,²⁰ we calculate that the average length scale of mixing x in the coalesced PCL/PLLA blend is 4.9 nm, while in the amorphous regions of the solution-cast blend this dimension is 7.4 nm. The expected radii of gyration for the PLLA and PCL molecular weights used here (3.5–5.0 nm) are comparable with the length scale of mixing calculated for the coalesced blend. On the other hand, the 7.5 nm length scale for the amorphous regions of the solution cast blend significantly

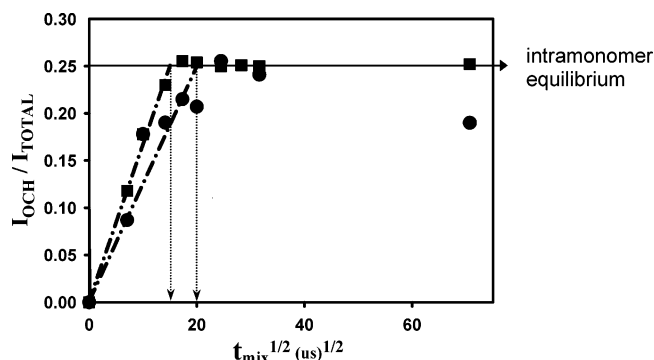


Figure 4. ¹H spin-diffusion curve from pure PLLA (■) vs PLLA in the coalesced blend with PCL (●), demonstrating a decrease in the spin-diffusion coefficient D upon blending. The last data point for the PLLA/PCL coalesced blend is already at the intermolecular equilibrium value, as previously seen in Figure 3.

exceeds the radii of gyration of both polymers. While the mixing of PCL and PLLA is truly molecular in the coalesced blend, additional phase segregation appears to occur between PCL and PLLA chains in the amorphous regions of the solution-cast blend. As expected, all dimensions are significantly smaller than the calculated upper limit from the average $T_{1H} = 1 \text{ s}$ value (55 nm).

Uncertainty in Blend Domain Size. In the calculations of minimum domain size above, a two-dimensional spin-diffusion model was used. Often, this is referred to as the morphology factor “ ϵ ”, which has values of 1, 2, or 3 for lamellar, cylindrical, or spherical morphology.²⁰ We have assumed that a lamellar morphology ($\epsilon = 1$) is unlikely for this amorphous blend, and the domain sizes reported above were obtained using $\epsilon = 2$, which represents the case for spin-diffusion in two orthogonal directions. However, it is well-known that spin-diffusion NMR is unable to discern the morphology of the sample independently; this is an assumption inherent to all spin-diffusion studies. Repeating the calculation using a possible spherical model for the discontinuous phase (spin diffusion in three orthogonal directions), we calculate the average minimum domain size x in the coalesced PCL/PLLA blend as 7.3 nm, while in the amorphous regions of the solution-cast blend this dimension is 11.3 nm, again below the limits from the $T_{1H} = 1 \text{ s}$ value (55 nm). In summary, the possible range of average minimum domain sizes for the two models gives 4.9–7.3 nm for the coalesced blend vs 7.5–11.3 nm for the solution-cast blend.

Change in Spin-Diffusion Coefficient D after Blending. One additional favorable aspect of the 2D Hetcor spin-diffusion method is the ability to determine spin-diffusion coefficients for the polymer in the blend and compare them to the values for the pure polymer prior to blending. By comparison, this would be analogous in theory to the measurement of T_g 's on a polymer in its pure vs mixed state. The spin-diffusion coefficient should reflect changes in molecular dynamics of the polymer after blending. Figure 4 shows that the time required to reach intramolecular polarization equilibration is shorter in pure, semicrystalline PLLA than it is for PLLA in the coalesced blend with PCL (15.5 $\mu\text{s}^{1/2}$ vs 20 $\mu\text{s}^{1/2}$, respectively). These values translate into spin-diffusion coefficients for the pure and mixed PLLA reflective of the expected increased chain mobility (and decreased D value) of PLLA when it forms an intimate

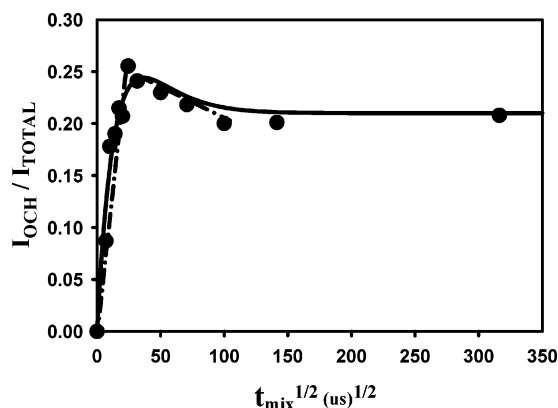


Figure 5. Two-component fit (solid line) of the coalesced PLLA/PCL spin-diffusion curve in Figure 3, with the short time response attributed to intramolecular polarization equilibration, and the long time component to interdomain spin diffusion.

(and amorphous) mixture with PCL having a much lower glass transition; we obtain $D_{\text{PLLA}}^{\text{pure}} = 2.1 \times 10^{-12} \text{ cm}^2 \text{ s}^{-1}$ and $D_{\text{PLLA}}^{\text{coal}} = 1.1 \times 10^{-12} \text{ cm}^2 \text{ s}^{-1}$. This reduction in D is consistent with X-ray diffraction data, which shows that almost all PLLA crystallinity is lost in the coalesced blend.

The value of $D_{\text{PLLA}}^{\text{pure}} = 2.1 \times 10^{-12} \text{ cm}^2 \text{ s}^{-1}$ is in agreement with our previous determinations of D 's based on intramonomer spin-diffusion.^{6,22} For the higher- T_g polycarbonate ($T_g = 140^\circ \text{C}$) and lower- T_g polyisobutylene ($T_g = -70^\circ \text{C}$), the previously reported spin-diffusion coefficients were 5.1×10^{-12} and $4.4 \times 10^{-14} \text{ cm}^2 \text{ s}^{-1}$, respectively. Since the PLLA T_g is intermediate between these two extremes ($T_g = 60^\circ \text{C}$), an intermediate value of D is expected.

Figure 5 shows the spin-diffusion curve for the coalesced PCL/PLLA blend, as in Figure 3, but with the addition of a two-component fit to the raw data. The purpose of this figure is to demonstrate that the linear least-squares analysis of the short-time data (to determine the intramolecular equilibration time) plus descending intensities to the intermolecular equilibration is an accurate representation of the total data.

Alternative Data Analysis Strategies. In this work we have extracted ^1H slices at specific ^{13}C shifts for construction of the spin-diffusion curves. Of course, as we showed in Figure 3 of ref 6, one could use also ^{13}C slices extracted at specific ^1H chemical shifts. However, there are some reasons why we feel this is not optimum. First, spinning-sideband intensities from large CSA peaks must be included in the data analysis. While this is not prohibitive, particularly for the high-speed spinning Lee–Goldburg Hetcor, it is an additional step requiring integration of multiple peak areas. More importantly, it potentially eliminates the useful “self-calibration” aspect of the experiment (based on the ^1H stoichiometry), in that ^{13}C slice intensities will not accurately reflect ^1H populations due to different heteronuclear transfer functions for the different carbon moieties (in the same way that traditional CP/MAS spectra are often not quantitative). A ^{13}C slice at a specific ^1H position is complicated by the fact that polarization transfer efficiency between a carbon and its directly bonded proton, for example, is different among the ensemble of isolated CH, CH_2 , and CH_3 groups in both the WIM- and LG-based steps. This potential problem is avoided by extracting a ^1H slice at

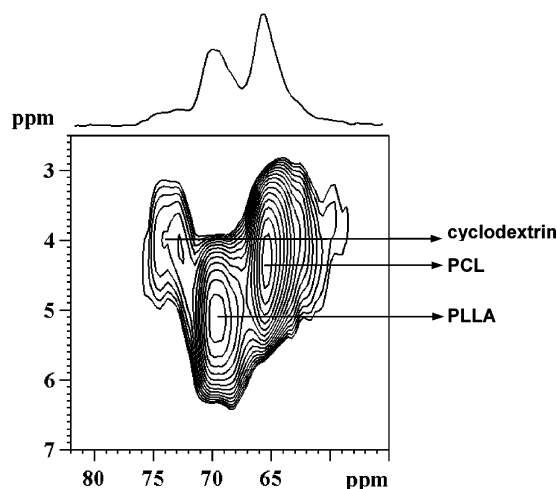


Figure 6. Expanded MP/WIM Hetcor plot of the OCH and OCH_2 region of the spectrum showing that the broad downfield (in the ^{13}C dimension) shoulder off the PLLA peak is clearly correlated to an upfield ^1H shift.

only one ^{13}C chemical shift position after the spin-diffusion time, since only *one* type of CH moiety is involved in reporting the extent of spin diffusion among *all* different proton types. This advantage is demonstrated by the fact that the expected ^1H intensity ratios, as required by the polymer structure, are obtained at each equilibrium point (intrachain or intermolecular) in Figure 3.

Relative Sensitivity for Trace Components. In Figure 1e, the PLLA OCH peak (peak f at 69 ppm) appears to broaden, and a downfield shoulder is evident at 72 ppm. Initially, we considered that the change in this peak shape for the coalesced blend, which was not observed in the solution blend spectrum of Figure 1d, might arise from some specific chemical interaction between the methine group of PLLA and carbonyl groups on PCL. However, close inspection of this region of the 2D Hetcor plot, obtained without any spin-diffusion time, reveals that this weak shoulder in the CP spectrum is a unique chemical moiety, based on its correlation to a new, unique ^1H chemical shift. No other carbon peaks in the spectrum share this ^1H shift, nor are there any other protons in either of the two polymers from which it could arise. Control experiments on pure cyclodextrin indicate that this “new” peak in the coalesced blend is simply the peak from trace amounts of α -cyclodextrin that were not completely removed by the DMSO washing step. However, its detection does raise an interesting point. Quantitative analysis of the coalesced blend using single-pulse ^{13}C excitation reveals that the amount of α -cyclodextrin remaining in the blend is only 2–3 mol %, and yet we are able to see a strong, well-resolved correlation in the Hetcor plot even in this crowded spectral region. The detection limit for a rigid structure like α -cyclodextrin is obviously lower than that for a highly mobile trace component. Nonetheless, the Hetcor approach, which is often ignored in materials analysis due to sensitivity concerns, provides the necessary data in this instance to clarify the questions arising from the one-dimensional CP/MAS data in Figure 1.

Conclusions

Two-dimensional spin-diffusion Hetcor experiments revealed that more intimately mixed blends of PCL and

PLLA could be prepared using inclusion compound coalescence techniques, relative to standard solution blending. The average minimum dimension for the amorphous coalesced PCL/PLLA blend was 4.9 nm, vs 7.4 nm for the amorphous regions of the semicrystalline PCL/PLLA blend prepared by dissolution in dioxane. The former dimension is comparable to the 4–5 nm radii of gyration for the particular PLLA and PCL polymers used, indicative of molecular level mixing in the coalesced blend. Individual spin-diffusion coefficients for PLLA and PCL chains in the blends were calculated on the basis of direct experimental measurement of the polymers in the blend. The magnitude of D was found to decrease by a factor of 2 for PLLA chains in the coalesced blend compared to the pure polymer. The extension of our previously published experimental strategy to these important biocompatible and biodegradable polyester blends demonstrates its general utility for characterizing multicomponent amorphous materials.

Acknowledgment. We gratefully acknowledge support of this work by the National Science Foundation (Grant DMR-0137968), the DuPont Science and Engineering Award program, the National Textile Center—U.S. Department of Commerce, and North Carolina State University. We thank Professor E. O. Stejskal for helpful discussions.

References and Notes

- (1) Smith, B. L.; Schaffer, T. E.; Viani, M.; Thompson, J. B.; Frederick, N. A.; Kindt, J.; Belcher, A.; Stucky, G. D.; Morse, D. E.; Hansma, P. K. *Nature (London)* **1999**, 399, 761.
- (2) John, J.; Mani, R.; Bhattacharya, M. *J. Polym. Sci., Polym. Chem.* **2002**, 40, 2003.
- (3) Ando, I.; Asakura, T. *Solid State NMR of Polymers*; Elsevier: Amsterdam, The Netherlands, 1998.
- (4) Schmidt-Rohr, K.; Spiess, H. W. *Multidimensional Solid-State NMR and Polymers*; Academic Press: New York, 1994.
- (5) Bovey, F. A.; Mirau, P. A. *NMR of Polymers*; Academic Press: New York, 1996.
- (6) Jia, X.; Wolak, J.; Wang, X.; White, J. L. *Macromolecules* **2003**, 36, 712.
- (7) Choi, N. S.; Kim, C. H.; Cho, K. Y.; Park, J. K. *J. Appl. Polym. Sci.* **2002**, 86, 1892.
- (8) Jeon, O.; Lee, S. H.; Kim, S. H.; Lee, Y. M.; Kim, Y. H. *Macromolecules* **2003**, 36, 5585.
- (9) Shuai, X.; Wei, M.; Porbeni, F. E.; Bullions, T.; Tonelli, A. E. *Biomacromolecules* **2002**, 3, 201.
- (10) Rusa, C.; Tonelli, A. E. *Macromolecules* **2000**, 33, 5321.
- (11) Burum, D. P.; Bielecki, A. *J. Magn. Reson.* **1991**, 94, 645.
- (12) van Rossum, B. J.; de Groot, C. P.; Ladizhansky, V.; Vega, S.; de Groot, H. J. M. *J. Am. Chem. Soc.* **2000**, 122, 3465.
- (13) Bronniman, C. E.; Ridenour, C. F.; Kinney, D. R.; Maciel, G. E. *J. Magn. Reson.* **1992**, 97, 522.
- (14) Wagler, T.; Rinaldi, P. L.; Han, C. D.; Chun, H. *Macromolecules* **2000**, 33, 1778.
- (15) Egger, N.; Schmidt-Rohr, K. S.; Blumich, B.; Domke, W. D.; Stapp, B. *J. Appl. Polym. Sci.* **1992**, 44, 289.
- (16) Mirau, P. A.; Yung, S. *Chem. Mater.* **2002**, 14, 249.
- (17) Kaplan, S. *Macromolecules* **1993**, 26, 1060.
- (18) White, J. L.; Mirau, P. A. *Macromolecules* **1994**, 27, 1648.
- (19) Li, S.; Rice, D. M.; Karasz, F. E. *Macromolecules* **1994**, 27, 2211.
- (20) Clauss, J.; Schmidt-Rohr, K.; Spiess, H. W. *Acta Polym.* **1993**, 44, 1.
- (21) Mellinger, F.; Wilhelm, M.; Spiess, H. W. *Macromolecules* **1999**, 32, 4686.
- (22) Wang, X.; White, J. L. *Macromolecules* **2002**, 35, 3795.

MA047838H